

the average with steep northwesterly or vertical dips (Fig. 1). The mineral lineation defined by elongated K-felspar grains on the plane of foliation is consistent and roughly downdip, implying thereby that shear movement was almost vertically upward (since the foliation plane is vertical to subvertical). The augen-gneiss has been traversed by numerous veins and bands (up to 12 cm wide) of a microgranodiorite concordant as well as discordant to the foliation.

Petrography and petrology: The Kurumda augen-gneiss consists of coarse grained porphyroblasts of K-felspar wrapped around by flakes of biotite and chlorite

TABLE I
Average modal compositions of Manda coarse biotite granodiorite, groundmass of augen-gneiss and chemical analysis of one sample (S/88) of augen-gneiss

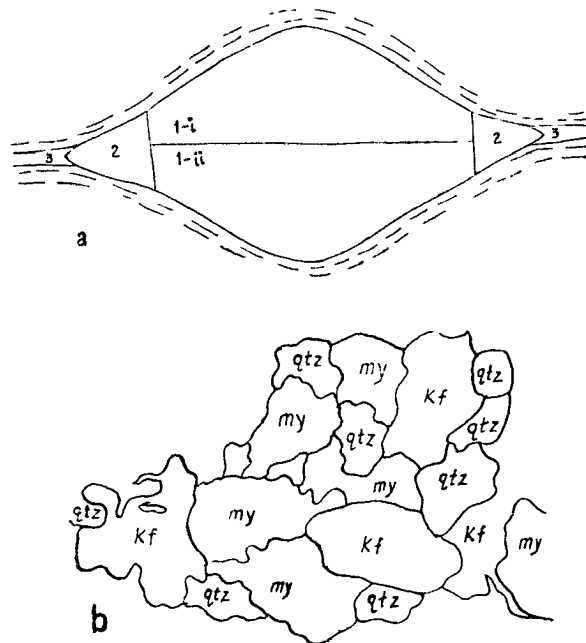
Minerals	Manda coarse Biotite granodiorite (Av. of 50 samples)	Groundmass of Augen-gneiss (Av. of 5 samples)	Oxides	Weight percentage oxides sample S/88
Plagioclase	55.1	50.1	SiO ₂	72.98
Quartz	29.0	31.5	Al ₂ O ₃	12.98
K-felspar	7.9	6.5	Fe ₂ O ₃	0.44
Biotite	3.8	6.2	FeO	1.44
Chlorite	2.3	1.5	MgO	0.08
Epidote	1.3	2.3	CaO	1.51
Opaque	0.1	0.5	K ₂ O	4.97
Non-opaque accessories sphene, apatite allanite	0.5	0.5	MnO	0.01
			TiO ₂	0.06
			P ₂ O ₅	0.48
Total			H ₂ O ₊	0.38
	100.0	100.1	H ₂ O ₋	0.67
Colour Index	8.0	11.5		

Analyst: A. Roy

together with plagioclase, quartz and other minor constituents. The average mineralogical composition of the groundmass of augen-gneiss, Manda coarse biotite granodiorite and the chemical analysis of one representative sample of augen-gneiss are shown in Table I.

In the augen-gneiss three compositionally different species of plagioclase occur: (i) large subhedral to euhedral grains of oligoclase, acid to basic in composition, similar to that in Manda coarse biotite granodiorite, (ii) clear thin rim of albite mantling the inclusions of oligoclase within K-felspar, and (iii) intermediate in composition between (i) & (ii).

The K-felspar augen: Three domains within one single twinned K-felspar eyeball can be recognised (Fig. 2). Domain 1 (i & ii) with numerous inclusions of myrmekitic plagioclase constitutes the major part while domain 2 represents the combination of dragged and pressure shadow domains, being composed of a massive aggregation of K-felspar and a little amount of quartz and relict plagioclase. Domain 3, the tail of the augen unit, is composed of fine to medium grained mosaic of K-felspar and quartz, both unaffected by granulation. The range of $2V_x$ values in the three domains - 1, 2 & 3, are $69^\circ - 90^\circ$, $58^\circ - 62^\circ$ and $44^\circ - 54^\circ$ respectively, and there is a progressive increase in the $2V_x$ values from the tail domain inward into the eyeball proper.



Kf-K-Felspar. my-Myrmekite. qtz-Quartz.

Figure 2 a. Sketch a typical K-felspar augen with different domains (1 × 5 cm).

b. Pressure shadow and dragged domains of the eyeball (× 25.4).

Taking into consideration that $2V$ of K-felspar is a function of composition and structural state, the K-felspar in the tail domain and in the dragged domain would represent an orthoclase ($2V_x < 60^\circ$), while the eyeball proper is somewhat ordered and microclitic ($2V_x = 69^\circ - 90^\circ$). But the porphyroblast probably grew as a monoclinic phase metastably since the mean $2V_x$ of all the measurements is low (72°). Following Ohta (1969) it may be suggested that the domain 1 crystallised during an intermediate period when stress was released, the domain 2 during the reactivation of differential movement, whereas the domain 3 crystallised in the last period of growth of the augen. It is clear that the K-felspar porphyroblasts, occurring as augens, grew in the solid state under componental movements along two sets of shear

planes in the granulated older Manda coarse biotite granodiorite (during the emplacement of younger microadamellite).

Genesis of the augen-gneiss: The two petrographic features with important bearings on the genesis of the augen-gneiss are:

(i) Composition of the groundmass material of the augen-gneiss closely approximates to that of the Manda coarse biotite granodiorite (Table I), as revealed from the Q-P-A diagram (Fig. 3) after F. Chayes (1957).

(ii) Presence of a third variety of plagioclase, albite to acid oligoclase in composition, in augen-gneiss in addition to types (i) & type (ii) (described earlier), the latter two varieties being also common to Manda coarse biotite granodiorite.

These observations indicate that the formation of K-felspar augen took place distinctly later than the emplacement of Manda coarse biotite granodiorite or its equivalent, the groundmass of the augen-gneiss and the third variety of plagioclase has been introduced within augen-gneiss during the formation of augen, from an younger microadamellite magma.

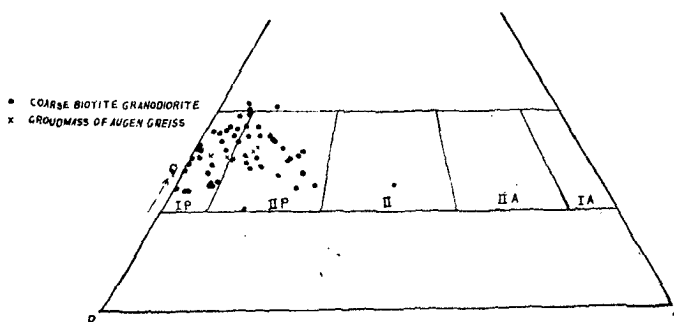


Figure 3. Q-P-A diagram after F-Chayes (1957) for the Manda coarse biotite granodiorite and the groundmass of augen-gneiss.

The most probable hypothesis on the genesis of the augen-gneiss is as follows:

The microgranodiorite bands and veins now found associated with augen-gneiss were originally emplaced as microadamellite melt from which a pegmatitic fraction (rich in SiO_2 , Al_2O_3 , K_2O , Na_2O , and with very little amount of CaO and total iron) was leached out. The leaching out of the pegmatitic fraction from microadamellite is further evidenced by the fact that the augen-gneiss is always associated with microgranodiorite and never with microadamellite which occurs as patches within only Manda coarse biotite granodiorite. It is likely that accompanying the crystallization of the microadamellite melt which intruded along the easily accessible foliation planes in the Manda coarse biotite granodiorite, there were shear movements; as a result, the residual liquid separated out of the already crystallised plagioclase-rich aggregates; the latter formed the microgranodiorite components within augen-gneiss, while the residual K-rich liquid was incorporated in the Manda coarse biotite granodiorite to produce the augen-gneiss.

The approximate composition of the postulated pegmatitic melt may be obtained by extrapolating the respective values of per cent oxides (as shown by straight lines in Fig. 4) for the average microgranodiorite and microadamellite, and assuming that there was no MgO in the pegmatitic melt (Table II).

Table II indicates that the derived pegmatitic melt was rich in SiO_2 and K_2O and deficient in Al_2O_3 , Na_2O , CaO and total iron. In an attempt to show that this melt by assimilation of Manda coarse biotite granodiorite has given rise to augen-gneiss, a simple graphical test was employed (Fig. 4) (Saha and Guha, 1968). As will be evident from Fig. 4, the composition of the analysed augen-gneiss (sample S/88) approximately fits in with a mixture of 16% coarse biotite granodiorite and 84% pegmatitic melt (leached out of the microadamellite). This assumption is supported by the fact that the proportion of the augens to groundmass in the analysed sample of augen-gneiss is around 80 : 20, as determined visually.

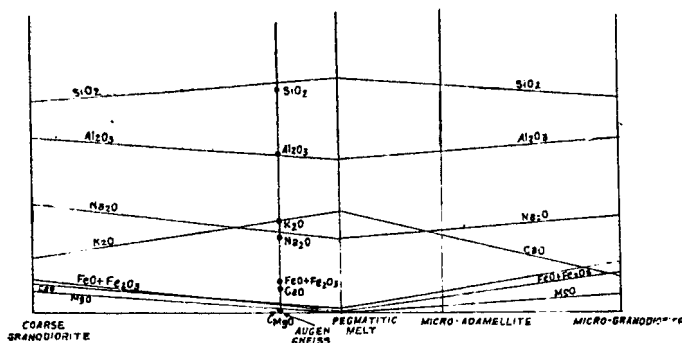


Figure 4. Graphical representation of the chemical composition of augen-gneiss, average microgranodiorite, average microadamellite and postulated pegmatitic melt.

TABLE II

Chemical composition of average microadamellite, average microgranodiorite and postulated pegmatitic melt (Data in weight percentage)

Oxides	Average Micro-adamellite	Average Micro-granodiorite	Pegmatitic melt
SiO_2	75.49	71.18	77.50
Al_2O_3	13.25	14.55	12.90
$\text{Fe}_2\text{O}_3 + \text{FeO}$	0.80	2.63	0.10
MgO	0.37	1.27	—
CaO	1.15	2.44	0.30
Na_2O	4.55	5.57	3.95
K_2O	4.23	1.98	5.30
MnO	0.01	0.04	—
TiO_2	0.13	0.14	—
P_2O_5	—	0.20	—

Conclusion: The data presented here thus supports the idea that shearing, accompanying the injection and crystallization of younger microadamellite, was responsible for the leaching out of pegmatitic melt from the partly crystallised magma

and the subsequent formation of K-felspar augens in augen-gneiss. Shear movement was continuing even after the formation of augens since augens themselves are found to have been sheared out in places. Augen-gneiss perhaps represents a mixture of pegmatitic melt and Manda coarse biotite granodiorite in variable proportions.

Acknowledgement: The author is grateful to Dr. A. K. Saha, Professor of Geology, Presidency College, Calcutta, under whose guidance this work was carried out.

REFERENCES

- CHAYES, F., (1957) Provisional re-classification of granites. *Geol. Mag.* v. 94, pp. 1-94.
- OHTA, Y., (1969) On the formation of augen structure. *Lithos*, v. 2, No. 2, pp. 109-132.
- SAHA, A. K., (1966) Magma tectonics of the northern part of Singhbhum Granite; a resume. *Proc. Symp. Tectonics. Nt. Inst. Sci. India*, pp. 59-76.
- SAHA, A. K. and GUHA, P. K., (1968) Genesis of the xenolithic granophyre dyke rocks within the Singhbhum granite. *Bull. Geol. Soc. Ind.* v. 5, no. 3, pp. 73-76.
- SEN, K. K., (1970) Modal composition variations in the granitic rocks around Kuldiha and Sulaipat in Mayurbhanj district, Orissa. *Quart. Jour. Geol. Min. & Met. Soc. Ind.* v. XLII, no. 1, pp. 1-15.

THE RHOMBOID PROTRACTOR AND ITS APPLICATION IN
THE CONSTRUCTION OF ISOMETRIC GEOLOGICAL PANEL DIAGRAMS

S. V. SRIKANTIA AND O. N. BHARGAVA

Chandigarh

Introduction: An isometric geological panel diagram consists of cross sections drawn on an isometric base. It represents an excellent method of geological illustration which enables a clearer understanding of complicated geological structures in three dimensions. An isometric section is actually a normal vertical section that has been rotated around 30° .

In normal vertical geological sections, the amount of dip of planar traces is usually plotted with the help of a rectangular protractor. However, in the case of isometric sections, wherein there is an introduction of fixed distortion of $+ \text{ or } - 30^\circ$, the rectangular protractor cannot be used for plotting the amount of dip of planar traces. In order to overcome this difficulty, the authors have designed a rhomboid protractor with the help of which the amount of 'distorted dip' can be directly plotted. In this paper, the design of the rhomboid protractor and the procedure for drawing the isometric geological panel diagrams are discussed.

Rhomboid protractor: The rhomboid protractor is simple in design and is actually the isometric representative of a rectangular protractor.

A standard rectangular protractor is a parallelogram which is divided into two equal halves each having 90° angles. When it is rotated around 30° its angular measurements are accordingly modified and it becomes a rhombus. The 90° on one half of the protractor is reduced to 60° and on another half is increased to 120° . This forms the rhomboid protractor. The 60° and 120° angles on either halves of the rhomboid protractor which are actually the isometric equivalents of 90° are